European Polymer Journal 88 (2017) 191–204

Contents lists available at ScienceDirect

European Polymer Journal

journal homepage: www.elsevier.com/locate/europolj

Polyampholyte hydrogels formed via electrostatic and hydrophobic interactions

Esra Su, Oguz Okay [*]

Istanbul Technical University, Department of Chemistry, 34469 Maslak, Istanbul, Turkey

ARTICLE INFO

Article history:
Received 12 December 2016
Received in revised form 18 January 2017
Accepted 22 January 2017
Available online 24 January 2017

Keywords:
Supramolecular hydrogels
Polyampholytes
Ionic interactions
Hydrophobic associations
Swelling
Mechanical properties

ABSTRACT

We introduce here a novel strategy to produce supramolecular polyampholyte hydrogels exhibiting pH sensitivity and anti-polyelectrolyte effect. The hydrogels were synthesized by photopolymerization of N,N-dimethylacrylamide (DMA) with equimolar amounts of the ionic monomers acrylic acid (AAc) and 4-vinylpyridine (4VP) under solvent-free condition. Instead of a chemical cross-linker, stearyl methacrylate (C18) was included into the comonomer feed to create hydrophobic associations. Both the electrostatic and hydrophobic interactions produce intermolecular linkages between the polymer chains acting as physical cross-link zones that are stable in water. Polyampholyte hydrogels are in a swollen state at $pH < 4$ and $pH > 6$ while they undergo a swelling-to-collapse transition between these pH values by adopting a collapsed conformation over a certain range of pH including their isoelectric points. This swelling behavior is a result of the pH difference between the inside and outside of the hydrogel, as demonstrated by the theory of swelling equilibrium. Rheological measurements indicate the reversible nature of the cross-link zones with finite lifetimes. Polyampholyte hydrogels containing 80–92% water exhibit Young's moduli between 18 and 58 kPa and sustain tensile strains up to 560%, while those prepared using a chemical cross-linker are brittle in tension. Cyclic mechanical tests show a large mechanical hysteresis and the existence of reversibly and irreversibly broken bonds under large strain.

1. Introduction

Polyampholytes are stimulus responsive materials containing oppositely charged functional groups. They received much attention in the past 60 years due to their biocompatibility, low toxicity, similarity to biological systems such as proteins and therefore, they have found various applications such as saline-resistant, anti-fouling and antibacterial materials [1–8]. At a high net charge density, polyampholyte molecules adopt an extended conformation in water due to the osmotic pressure of mobile counterions confined inside the polymer coil to achieve the electroneutrality. As the net charge density decreases, the conformation of the molecules changes from extended to collapsed coils because of the decrease of mobile counterion concentration and strong electrostatic attractive forces between oppositely charged segments. The addition of salt shields the electrostatic interactions in charge-balanced polyampholyte molecules leading to the expansion of polymer coils known as the anti-polyelectrolyte behavior. It was also shown that hydrophobically modified polyampholytes form intermolecular

---

[*] Corresponding author.
E-mail address: okayo@itu.edu.tr (O. Okay).

http://dx.doi.org/10.1016/j.eurpolymj.2017.01.029

hydrophobic associations in aqueous solutions [9–12]. Thus, they combine the properties of hydrophobically modified non-ionic polymers and polyampholytes making them effective viscosity enhancers in brine solutions.

Hydrogels mimicking the solution properties of polyampholyte molecules have been prepared by copolymerization of ionic monomers possessing cationic and anionic charges in the presence of a chemical cross-linker [13–22]. Strong polyampholyte hydrogels bearing permanent charges have a fixed net charge and therefore they exhibit pH-independent swelling behavior. Thus, the net charge of such hydrogels can only be varied by changing the comonomer ratio in the feed. In contrast, the net charge of weak polyampholyte hydrogels possessing functional groups like amines and carboxylic acids varies with the pH leading to pH-dependent swelling behavior, swelling-to-collapse transition, and anti-polyelectrolyte behavior in aqueous solutions [15,22]. Although polyampholyte hydrogels have a number of technological applications [8,19–21], they are mechanically weak materials due to the covalently cross-linked network structure, preventing dissipation of the crack energy and thus leading to their fracture under low stresses. Recently, supramolecular hydrophobically modified polyampholyte hydrogels were prepared by copolymerization of acrylamide and acrylic acid in the presence of a cationic surfmer [23]. Although pH-dependent swelling characteristics and mechanical properties of the hydrogels were not reported, they exhibit shape-memory effects and thermoplasticity. Gong et al. prepared high-toughness polyampholyte hydrogels in the absence of a chemical cross-linker by random copolymerization of oppositely charged ionic monomers at a high concentration around the zero net charge point [24,25]. It was shown that the randomness of charges leads to the formation of multiple ionic bonds with a wide distribution of strengths. While the strong bonds act as permanent cross-links, the weak bonds acting as reversible sacrificial bonds easily fracture under a low stress and hence, dissipate energy to prevent crack propagation [24]. Although the hydrogels exhibit a high mechanical strength, they do not display typical swelling characteristics of polyampholyte hydrogels due to their low water contents, e.g., 52–61 wt%, and the presence of strong electrolyte functional groups.

Here, we describe preparation of supramolecular polyampholyte hydrogels exhibiting pH-dependent swelling behavior, swelling-to-collapse transition, and anti-polyelectrolyte property. The hydrogels were prepared by photopolymerization of the non-ionic monomer N,N-dimethylacrylamide (DMA) with the ionic monomers acrylic acid (AAc) and 4-vinylpyridine (4VP) under solvent-free condition (Scheme 1a). The choice of these monomers as building blocks of supramolecular hydrogels is due to the fact that both poly(DMA) and poly(4VP) are well known proton acceptor polymers able to form interpolymer complexes with several proton donor polymers such as poly(AAc) [26]. Moreover, it was shown that poly(AAc) and poly(4VP) form hydrogen-bonded complexes in aqueous solutions through the cooperative hydrogen-bonding interactions [27]. We used equimolar amounts of AAc and 4VP between 10 and 20 mol% in the gel preparation together with the hydrophobic monomer stearyl methacrylate (C18) at a concentration of 2 mol% to create hydrophobic associations [28,29] (Scheme 1b). As will be seen below, both the electrostatic interactions between AAc and 4VP segments carrying weak anionic and cationic groups, respectively, and the hydrophobic interactions between C18 segments produce intermolecular linkages acting as physical cross-link zones that are stable in water. Hydrogels are in swollen states at pH < 4 and pH > 6 while they undergo a collapse transition between these pH values. The results also show that polyampholyte hydrogels adopt a collapsed conformation over a range of pH including their isoelectric points. This finding is in agreement with the prediction of the classical Flory-Rehner swelling theory coupled to the Donnan equilibrium and indicates different pHs between the inside and outside of the gel phase. Rheological measurements reveal reversible nature of the cross-link zones in the hydrogels with finite lifetimes. The hydrogels containing 80–92% water exhibit Young's moduli between 18 and 58 kPa and sustain tensile strains up to 560%, while those prepared using a chemical cross-linker are brittle in tension. Cyclic mechanical tests show a large mechanical hysteresis and the existence of reversibly and irreversibly broken bonds under large strain.

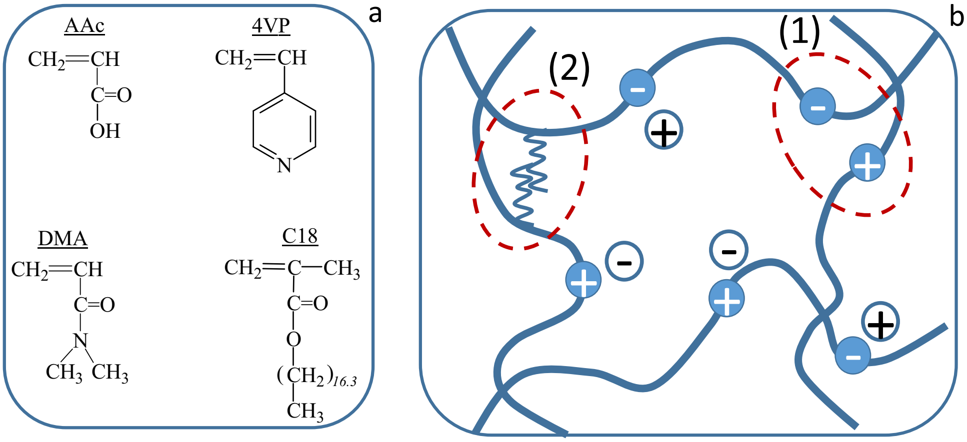

Scheme 1. (a) Structure of the monomers used in the preparation of polyampholyte hydrogels. (b) Scheme showing intermolecular electrostatic interactions between ionized AAc and 4VP segments (1), and hydrophobic interactions between C18 segments of polyampholyte hydrogels (2).

2. Materials and methods

2.1. Materials

Acrylic acid (AAc, Merck) was freed from its inhibitor by passing through an inhibitor removal column purchased from Sigma-Aldrich. Commercially available stearyl methacrylate (C18, Sigma-Aldrich) consists of 65% *n*-octadecyl methacrylate and 35% *n*-hexadecyl methacrylate. 4-vinylpyridine (4VP), N,N-dimethylacrylamide (DMA), N,N'-methylenebis(acrylamide) (BAAm), 2-Hydroxy-4′-(2-hydroxyethoxy)-2-methylpropiophenone (Irgacure 2959), and NaCl obtained from Sigma-Aldrich were used as received.

2.2. Hydrogel preparation

The hydrogels were prepared by bulk photopolymerization of the monomers DMA, AAc, 4VP, and C18 at 23 ± 2 °C in the presence of 0.2 mol% Irgacure 2959 photoinitiator under UV light at 365 nm. Equimolar amounts of the ionic monomers AAc and 4VP between 10 and 20 mol% were used in the gel preparation while the amount of C18 in the comonomer feed was fixed at 2 mol%. For comparison, the hydrogels were also prepared in the presence of BAAm cross-linker instead of C18. In the following, the hydrogels are coded by x/x where x represents the mole percent of AAc or 4VP in the comonomer feed. For example, 15/15 hydrogel was prepared from a comonomer feed consisting of 15 mol% AAc, 15 mol% 4VP, 2 mol% C18, and 68 mol% DMA. Moreover, the hydrogel coded as 0/0 in the following paragraphs was prepared in the absence of the ionic monomers and thus, it contains poly(DMA) network chains having 2 mol% hydrophobic C18 segments. To illustrate the synthetic procedure, we give details for the preparation of 15/15 hydrogels: DMA (3.323 g), 4VP (0.818 g), AAc (0.533 g), and C18 (0.324 g) were mixed at room temperature and stirred for 15 min to obtain a homogeneous solution. After addition of Irgacure 2959 (0.025 g) and stirring for 1–2 min, nitrogen gas was bubbled through the homogeneous solution for 30 min to eliminate oxygen. The solution was then transferred into several rectangular plastic molds (250 × 13 × 0.5 mm) and the molds were placed in a UV reactor to conduct the polymerization reactions under UV light at 365 nm for 24 h.

2.3. Swelling and gel fraction measurements

The copolymer samples after preparation were cut into samples of about 10 mm in length. Then, each sample was immersed in a large excess of distilled water at 24 ± 0.5 °C for at least 2 days by replacing water several times to extract any soluble species. Visual observations revealed that the copolymers after synthesis were green in color while the color changed to slight yellow or transparent after their equilibrium swelling in water, but reversibly, drying of the gel samples resulted in green colored samples (Fig. S1). The swelling equilibrium was tested by weighing the gel samples. The equilibrium swollen hydrogel samples in distilled water were than taken out of water and freeze dried. The gel fraction W_g, that is, the conversion of monomers to the water-insoluble polymer was calculated from the masses of dry polymer network and from the comonomer feed. The equilibrium weight swelling ratio q_w was calculated as $q_w = m/m_{dry}$ where m is the mass of the equilibrium swollen gel sample, and m_{dry} is the hydrogel mass after freeze-drying. From the swelling ratios the water content of the hydrogels was calculated as $H_2O\% = 10^2(1 - 1/q_w)$. We have to mention that the pH of the distilled water with a conductivity of below 0.055 μS used in the swelling tests was slightly acidic (pH = 5.4 ± 0.5) at the swelling equilibrium of hydrogels, which we attribute to the CO_2 absorption from the air. Swelling measurements were also carried out in water and in aqueous 0.1 M NaCl solutions at various pHs between 2 and 10, adjusted by adding dilute HCl or NaOH solutions. pH measurements were conducted using WTW inoLab pH meter with WTW SenTix 41 pH electrodes calibrated using three buffer solutions of varying pH between 4 and 10.

2.4. Characterization of the network chains

Although the hydrogels were insoluble in water, they could be solubilized in water if the hydrophobic monomer C18 is not included in the comonomer feed. This provided structural characterization of the polymer chains building the physical network of the hydrogels. For this purpose, 10/10-, 15/15-, and 20/20-copolymers were first prepared as described above but in the absence of C18 monomer, followed by dissolving the copolymers in water to obtain a polymer solution of concentration around 0.1 g·mL^{-1}. To separate the unreacted monomers and the initiator, the polymer solutions were dialyzed using dialysis tubing (3500 MWCO, Snake Skin, Pierce) for 3 days against water that was changed three times a day. The solutions were then taken out of the tubing and freeze dried.

The molecular weight of the copolymers was determined using gel permeation chromatograph (GPC) measurements performed at room temperature with a setup consisting of a pump (Agilent 1100), a refractive index detector (Agilent 1100s), and Waters Ultrahydrogel 250 and 500 columns. The polymer solutions were prepared by dissolving 10 mg of the copolymers each in 7 mL phosphate buffer at pH = 7 followed by filtration of the solution through Nylon membrane filters (pore size = 0.2 μm). Phosphate buffer (pH = 7) was used as eluent at a flow rate of 0.7 mL min^{-1}. Calibration with linear polyethylene oxide standards was used to estimate molecular weights.

AAc content of the copolymers was determined using European Disposables and Nonwoven Association (EDANA) test method 470.2-0.2, which bases on the titration of the polymer solution with 0.1 M NaOH and back titration with 0.1 M HCl. To determine 4VP content of the copolymers, ^{1}H NMR spectra of the copolymers dissolved in D_2O (10 mg·mL^{-1}) were recorded at room temperature on an Agilent VNMRS 500 spectrometer at 500 MHz using tetramethylsilane as internal standard. Fig. 1a shows typical NMR spectrum of 15/15-copolymer in D_2O. The peaks at δ = 8.3–8.5 ppm (a) and 7.2 ppm (b) are assigned to meta- and ortho-protons of pyridine ring, respectively, while the peaks between 2.8 and 3.0 ppm characterize the methyl groups of DMA units (c). 4VP content of the copolymers was determined from the area ratio of meta-protons to methyl proton peaks.

2.5. Rheological experiments

Polyampholyte hydrogel samples equilibrium swollen in water were subjected to dynamic experiments at 20 °C between the parallel plates of the rheometer (Gemini 150 Rheometer system, Bohlin Instruments) equipped with a Peltier device for temperature control. The upper plate (diameter 20 mm) was set at a distance of 1000–1375 μm, depending on the swelling degree of the hydrogels. During all measurements, a solvent trap was used to minimize the evaporation. Frequency sweep tests were carried out between the angular frequencies ω 0.06 and 300 rad·s^{-1} at a deformation amplitude γ_o of 0.01.

2.6. Mechanical tests

Uniaxial compression and elongation measurements were performed at 23 ± 2 °C on swollen hydrogel samples on a Zwick Roell test machine with 500 N load cell. Load and displacement data were collected during the experiments. The Young's modulus E was calculated from the slope of stress–strain curves between 5 and 15% deformations. For uniaxial compression measurements, rectangular hydrogel samples of 3 mm in width and 2 ± 0.5 mm in length were compressed at a strain rate of 8×10^{-3} s^{-1}. Before the test, an initial compressive contact to 0.01 ± 0.002 N was applied to ensure a complete contact between the gel and the plates. The stress was presented by its nominal σ_{nom} or true values σ_{true} (=$\lambda\sigma_{nom}$), which are the forces per cross-sectional area of the undeformed and deformed gel specimen respectively, while the compressive strain is given by λ, the deformation ratio (deformed length/initial length). The strain is also given by ε, the change in the sample length relative to its initial length, i.e., $\varepsilon = 1 - \lambda$ or $\varepsilon = \lambda - 1$ for compression and elongation, respectively. We have to mention that the supramolecular gel samples did not break even at a strain of about 100% compression, and therefore, the nominal stress σ_{nom} increased continuously with increasing strain. This is illustrated in Fig. 1b for the 15/15-hydrogel showing the dependences of σ_{nom} and σ_{true} on the compressive strain ε. Although σ_{nom}–ε plot continuously increases, the corresponding σ_{true}–ε plot passes through a maximum indicating the onset of a microscopic failure in the gel specimen [30]. Therefore, the nominal fracture stress σ_f and the compression ε_f at failure were calculated from the maxima in σ_{true}–ε plots, as shown by the dashed lines in Fig. 1b. The cyclic compression tests were conducted at a constant strain rate of 8×10^{-3} s^{-1} to a maximum compression ratio, followed by retraction to zero force and a waiting time of 1 min until the next cycle of compression. Uniaxial elongation measurements were performed on dumbbell-shaped hydrogel samples with the standard ISO-37 type 2 (ISO

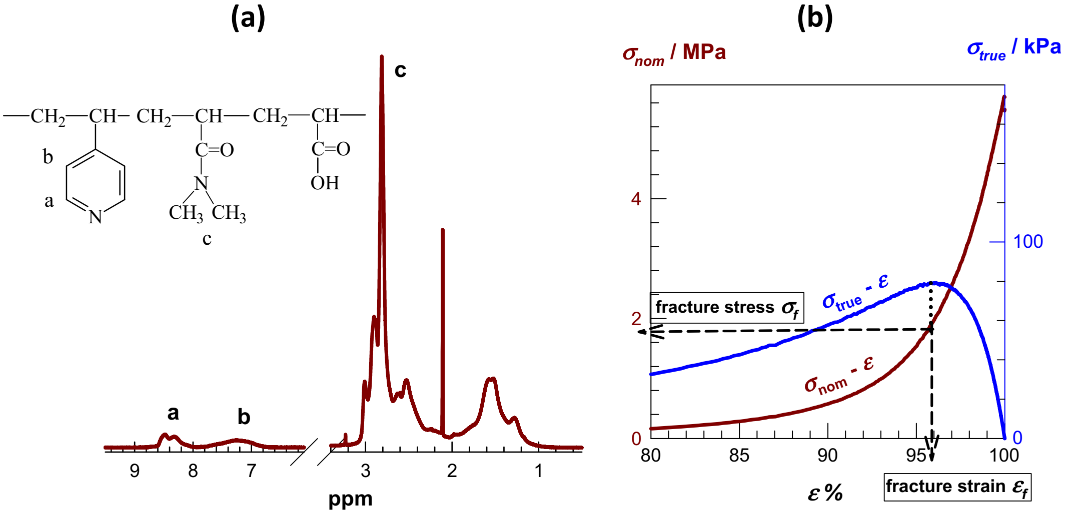

Fig. 1. (a) ^{1}H NMR spectrum of 15/15-copolymer in D_2O. (b) Typical stress–strain curves of 15/15-hydrogel specimens under compression as the dependences of nominal σ_{nom} (dark red curve) and true stresses σ_{true} (blue curve) on the compressive strain ε. Dashed lines represent calculations of the fracture stress and fracture strain from the maximum in the σ_{true}–ε curve. (For interpretation of the references to color in this figure legend, the reader is referred to the web version of this article.)

527-2) under following conditions: Strain rate = $1.7 \times 10^{-2}\ s^{-1}$; sample length between jaws = 50 ± 2 mm. Cyclic elongation tests were conducted as the compression cycles except that the strain rate was set to $1.7 \times 10^{-2}\ s^{-1}$.

3. Results and discussion

Supramolecular polyampholyte hydrogels were synthesized by bulk photopolymerization of the monomers DMA, AAc, 4VP, and C18 under solvent-free condition followed by swelling of the resulting copolymers in water. Because DMA is a liquid at room temperature and totally miscible with the other monomers together with the initiator Irgacure 2959, the bulk polymerization is a simple supramolecular approach for preparing polyampholyte hydrogels. Preliminary experiments were carried out to optimize the concentrations of the ionic monomers AAc and 4VP as well as the hydrophobic monomer C18 in the comonomer feed. At AAc or 4VP concentrations higher than 20 mol%, water-insoluble physical gels could not be obtained while at high C18 concentrations (>2 mol%), the hydrogels formed exhibited a weak pH-dependent swelling behavior (Fig. S2). In the following, we will mainly discuss the results obtained using a comonomer feed composition consisting of 2 mol% C18 and equimolar amounts of AAc and 4VP between 10 and 20 mol%.

3.1. Gel fraction and swelling properties

After a polymerization time of 24 h, the copolymers formed were insoluble in water with a gel fraction W_g of around 0.90 indicating that ~90 wt% of the monomers in the feed are converted into water-insoluble copolymers (Table 1). W_g slightly increases with increasing ionic comonomer content in the feed which we attribute to increasing extent of intermolecular electrostatic interactions between copolymer chains. Although the hydrogels were insoluble in water, they could be solubilized if the hydrophobic comonomer C18 is not included in the comonomer feed. This highlights that not only the electrostatic interactions between the polymer chains but also the hydrophobic associations between C18 segments are required for the preparation of hydrogels that are stable in water. The solubilization of the hydrogels prepared without the hydrophobic monomer C18 also provided the structural characterization of the network chains. GPC measurements conducted on aqueous solutions of the copolymers give an average molecular weight of $1.5 \pm 0.5 \times 10^6\ g \cdot mol^{-1}$ with a molar mass dispersity of 1.15. This high molecular weight is attributed to the solvent—free condition used in the polymerization procedure. Moreover, we have to note that this GPC-determined molecular weight and molar mass dispersity are only estimated values based on the PEO standards. Determination of AAc and 4VP repeat unit contents of the network chains by titration and NMR techniques, respectively, gives slightly higher values as compared to their amounts in the feed (Table 1). However, AAc to 4VP molar ratio R in the network chains is close to unity, i.e., between 0.88 and 0.90 (Table 1), indicating that their ionized concentrations are around the zero net charge point

Table 1 also shows that the copolymers swell 5–13 times their dry mass in distilled water corresponding to a water content between 80 and 92 wt% that increases with decreasing amount of the ionic monomers in the feed. Decreasing water content of the hydrogels on raising the ionic monomer content indicates that the swelling degree is governed by the extent of electrostatic interactions. For comparison, we also prepared 15/15-hydrogel using 2 mol% chemical cross-linker BAAm, instead of the hydrophobic monomer C18, which is denoted by 15/15xl (Table 1). As compared to the supramolecular 15/15-hydrogel, 15/15xl-hydrogel exhibits a complete gel fraction but the lowest water content of 78 wt%.

Swelling measurements were also conducted on polyampholyte hydrogels immersed in aqueous solutions of various pH as well as in 0.1 M NaCl solution. In Fig. 2a, the equilibrium swelling ratio q_w of the hydrogels is plotted against the pH of the solution. Open symbols in the figure are the results obtained using 15/15xl-gel specimens prepared using the chemical cross-linker BAAm. The chemical gel exhibits only a slight pH-dependence while supramolecular hydrogels undergo up to 2-orders of magnitude change in the gel mass depending on the pH of the solution. The pH at zero net charge in the hydrogels, i.e., the isoelectric point pI corresponds to the pH at which the numbers of ionized AAc and 4VP segments are equal. Thus, the condition of isoelectric point is given by $\alpha R = \beta$, where α and β are the dissociation degrees of AAc and 4VP segments, respectively, defined as $\alpha = [1 + 10^{(pKa-pH)}]^{-1}$ and $\beta = [1 + 10^{(pKb+pH-14)}]^{-1}$. The values of $pK_a = 4.25$ and $pK_b = 8.77$ taken from previous studies [31,32], together with the R ratios listed in Table 1, we calculated the isoelectric point pI as 4.86, 4.82,

Table 1
Ionic segment contents, swelling and mechanical properties of polyampholyte hydrogels. x_{AAc} and x_{4VP} = mole fractions of AAc and 4VP segments in the copolymers, respectively, R = AAc to 4VP molar ratio in the network chains. W_g = gel fraction. q_w = equilibrium weight swelling ratio in water. $H_20\%$ = water content (in wt%). E = Young's modulus (average of tensile and compression test results), σ_f = fracture stress, ε_f = deformation at break. $\lambda > 1$ and $\lambda < 1$ indicate the results obtained from tensile and compression tests, respectively. Standard deviations are given in the parenthesis.

Code	x_{AAc}	x_{4VP}	R	W_g	q_w	H_2O %	E / kPa	σ_f / kPa		ε_f%	
								$\lambda > 1$	$\lambda < 1$	$\lambda > 1$	$\lambda < 1$
10/10	0.14 (0.01)	0.16 (0.01)	0.88	0.86 (0.01)	13 (2)	92 (1)	18 (1)	62 (6)	1712 (50)	530 (10)	96 (0)
15/15	0.21 (0.01)	0.23 (0.01)	0.91	0.87 (0.01)	8 (0)	88 (1)	20 (1)	66 (2)	1652 (86)	560 (20)	96 (0)
20/20	0.23 (0.04)	0.28 (0.01)	0.82	0.90 (0.03)	5.0 (0.2)	80 (1)	58 (3)	110 (16)	419 (82)	310 (10)	87 (1)
15/15xl	–	–	–	1.0 (0)	4.5 (0.1)	78 (0)	536 (13)	Brittle	738 (61)	Brittle	60 (5)
0/0	0	0	–	1.0 (0)	11.8 (0.4)	92 (0)	12 (1)	25 (4)	1740 (116)	420 (40)	96 (0)

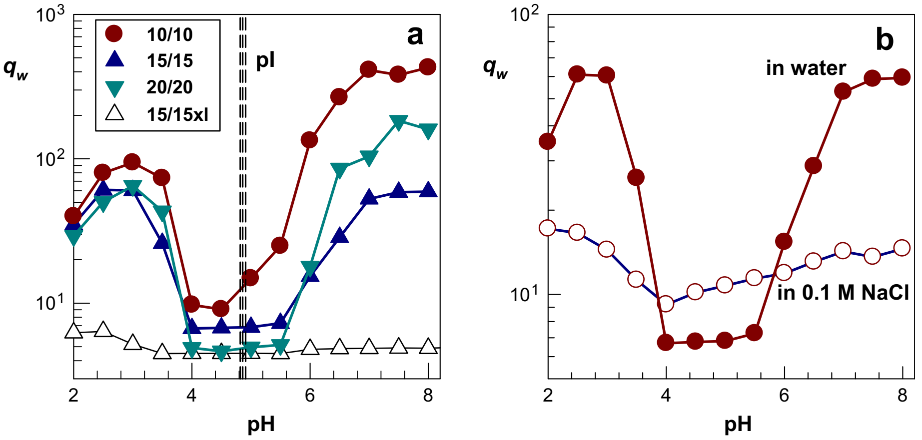

Fig. 2. (a) pH dependence of the equilibrium swelling ratio q_w of polyampholyte hydrogels. The isoelectric points are indicated by the vertical dashed lines. (b) q_w versus pH plots of 15/15-hydrogel measured in water (filled symbols) and in aqueous 0.1 M NaCl solution (open symbols).

and 4.91 for 10/10-, 15/15-, and 20/20-hydrogels, respectively [33], which are close to $pI = 4.74$ calculated for $R = 1$. The vertical dashed lines in Fig. 2a represent pI values of the hydrogels. It is seen that although the hydrogels are in a collapsed conformation at the calculated pI values, they remain collapsed over a certain range of pH. The collapsed plateau region for 15/15- and 20/20-hydrogels is over a pH range of 4.0–5.5, while for 10/10-hydrogel this pH range is between pH 4.0 and 4.5. Moreover, the water content of the hydrogels in the collapsed region decreases with increasing amount of the ionic segments in the hydrogels. For instance, at pH = 4.5, the water contents are 89, 85, and 78 wt% for 10/10-, 15/15-, and 20-20-hydrogels, respectively. As the pH is decreased or increased outside the plateau range, the hydrogels start to swell due to the fact that they behave as cationic or anionic polyelectrolytes, respectively. The results also show that the hydrogels again deswell after attaining a maximum degree of swelling at pH = 3. Because pH $\leqslant 3$ corresponds to H^+ concentration of $\geqslant 10^{-3}$ M, this high H^+ ion concentration in the solution seems to suppress the osmotic pressure of mobile counterions confined in the polyampholyte network leading to gel deswelling, as observed in polyelectrolyte hydrogels immersed in aqueous salt solutions [34].

Fig. 2b shows the swelling ratio q_w of 15/15-hydrogel samples immersed in water (filled symbols) and in 0.1 M NaCl solution (open symbols) plotted as a function of pH of the solutions. In contrast to the strong pH-dependent swelling behavior of 15/15- hydrogel in water, only a slight pH dependence and a weak minimum in q_w at pH = 4 can be seen when it is immersed in NaCl solution. This is attributed to the decrease of the concentration difference of mobile counterions between in and out of the hydrogel when immersed in salt solution instead of water, reducing the ionic osmotic pressure of the gel. As a consequence, except within the plateau region, the hydrogel is less swollen in salt solution as compared in water. However, within the plateau regime the hydrogel exhibits a larger degree of swelling in 0.1 M NaCl solution as compared to water. This anti-polyelectrolyte behavior observed in the plateau region is due to the reduction of electrostatic attractions between charged AAc and 4VP segments in the presence of salt ions and thus inducing gel swelling. The swelling behavior of the hydrogels summarized above will be discussed in Section 3.3 within the framework of Flory-Rehner theory of equilibrium swelling.

3.2. Rheological and mechanical properties

Dynamic properties of the hydrogels were investigated by rheometry using oscillatory deformation tests. Fig. 3a and b compares the viscoelastic spectra of 15/15- and 15/15xl-hydrogels prepared in the presence of the hydrophobic monomer C18 and the chemical cross-linker BAAm, respectively. Here, the storage modulus G' (filled symbols), loss modulus G'' (open symbols), and loss factor $\tan\delta$ (lines) of the hydrogels are plotted against the angular frequency ω. The storage modulus of chemically cross-linked polyampholyte hydrogel (15/15xl) is frequency independent and the loss factor remains below 0.1 corresponding to solid-like behavior. In contrast, the supramolecular 15/15-hydrogel exhibits frequency-dependent storage modulus and a loss factor above 0.1 demonstrating the temporary nature of the physical cross-links with a finite lifetime of the order of seconds to milliseconds. The viscoelastic spectra of 10/10- and 20/20-hydrogels given in Fig. 3c and d reveal that increasing ionic comonomer content also increases the storage modulus while the loss factor decreases indicating the contribution of the electrostatic interactions between AAc and 4VP segments to the elasticity of the hydrogels. This finding is in accord with increasing gel fraction and decreasing water content of the hydrogels on raising the amount of the ionic segments (Table 1).

The dynamic nature of cross-links in supramolecular hydrogels resulted in an enhancement in the mechanical properties when compared with the chemically cross-linked ones. This is illustrated in Fig. 4a where the compressive stress σ_{nom} is plot-

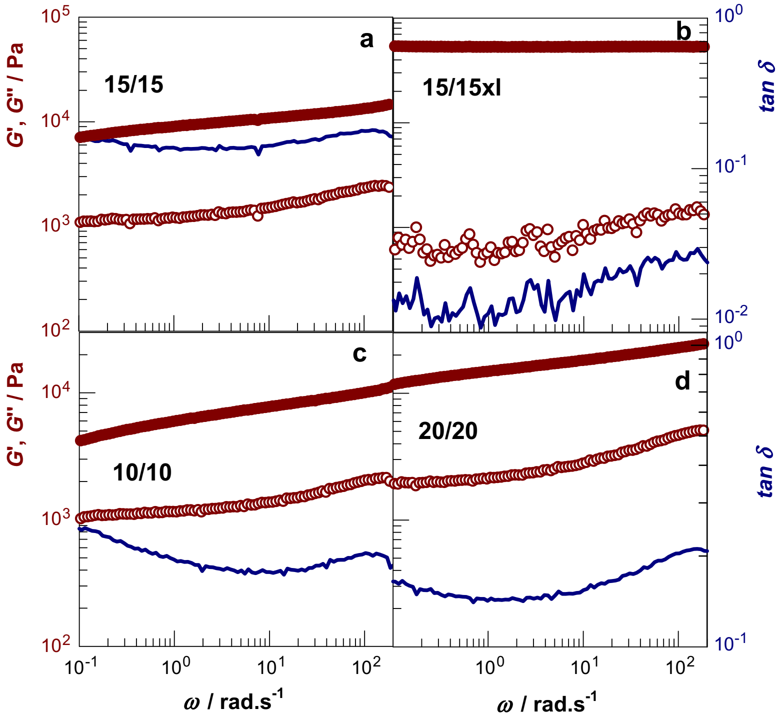

Fig. 3. The storage modulus G' (filled symbols), loss modulus G'' (open symbols), and loss factor $\tan\delta$ (lines) of polyampholyte hydrogels plotted against the angular frequency ω. The codes of the hydrogels are indicated. $\gamma_o = 0.01$. Temperature = 20 °C.

ted against the compressive strain ε for 15/15- and 15/15xl- hydrogels. The chemically cross-linked hydrogel sample (15/15xl) fractures at 60 ± 5% compression under 0.74 ± 0.06 MPa stress while the corresponding supramolecular 15/15-hydrogel sample sustains up to 96% compression at 1.65 ± 0.09 MPa stress. As detailed in the experimental section, the fracture stress and strain were calculated from the maxima of true stress σ_{true} – strain curves, corresponding to the onset of a microscopic failure in the gel sample (Fig. 1b). In the chemically cross-linked 15/15xl gel samples, this point also corresponded to the onset of macroscopic failure, while 15/15-hydrogels remained stable even under 99% compression (Fig. 1b). Photographs in Fig. 5 also demonstrate how the supramolecular polyampholyte hydrogel maintains its macroscopic integrity under 99% compression (bottom panel), while the chemically cross-linked hydrogel fractures into numerous smaller pieces (upper panel). Moreover, chemically cross-linked 15/15xl hydrogel was brittle in tension and broke at the start of tensile tests while 15/15-hydrogel could be stretched about 7 times its original length. The dashed curve in Fig. 4a represents the stress-strain data of 0/0-hydrogel sample prepared in the absence of the ionic comonomers and thus, it consists of poly(DMA) chains containing 2 mol% C18. This curve closely matches to that of 15/15-hydrogel revealing that the improvement in the mechanical properties is due to the replacement of the chemical cross-linker BAAm with the hydrophobic monomer C18.

Fig. 4b shows stress-strain curves of 10/10- and 20/20-hydrogels under compression (left) and elongation (right). The characteristic tensile and compression data of the hydrogels, i.e., the Young's modulus E, the fracture stress σ_f, and strain at break ε_f are collected in Table 1. The lowest modulus E was measured for 0/0-hydrogel prepared in the absence of the ionic monomers and it increases with increasing ionic segment content of the hydrogels. The largest modulus and the compressive fracture stress are 58 ± 3 kPa and 1.71 ± 0.05 MPa, respectively, that were obtained for 20/20- and 10/10-hydrogels, respectively. We have to mention that the modulus E and the fracture stress σ_f of polyampholyte hydrogels could be further increased by increasing the amount of the hydrophobic monomer C18 in the comonomer feed. For instance, Fig. 4c shows compressive stress-strain curves of 15/15-hydrogels formed at various C18 levels between 2 and 10 mol%. The modulus E increases from 20 ± 1 kPa to 1.1 ± 0.1 MPa with increasing C18 content from 2 to 10 mol%. The hydrogels formed at 10 mol% C18 content sustain up to 13.5 ± 0.1 MPa fracture stress. Thus, the fracture stress of 15/15-hydrogel formed at 2 mol% C18 could be increased by a factor of 8.2 when the hydrophobe level is increased to 10 mol%. However, mechanically stronger hydrogels thus formed by increasing the extent of hydrophobic interactions exhibited a low degree of swelling in water and weak pH-dependent swelling behavior (Fig. S2).

To understand whether the dynamic intermolecular bonds in the hydrogels break and reform reversibly under strain, we investigated the large strain properties of the hydrogels by cyclic compression and tensile tests. The tests were carried out by compressing and stretching the gel samples up to a maximum strain ε_{max} followed by immediate retraction to zero displace-

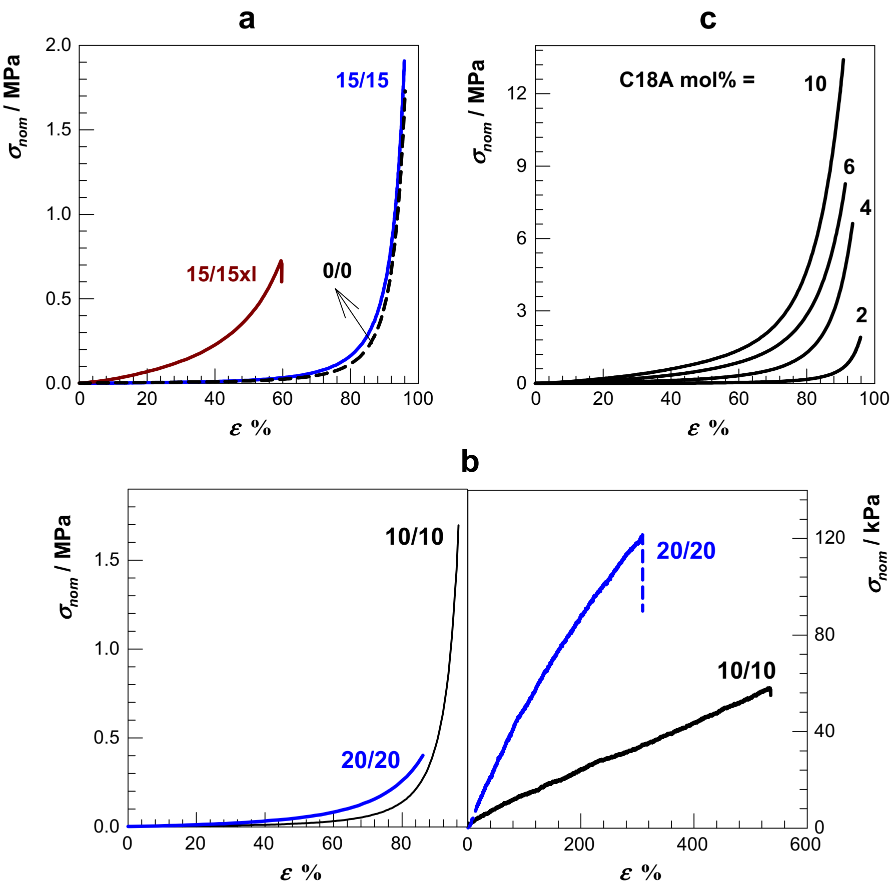

Fig. 4. Stress-strain curves of polyampholyte hydrogels as the dependence of nominal stress σ_{nom} on the strain ε. (a) Compressive stress–strain curves of chemically (15/15xl) and physically cross-linked hydrogels via hydrophobic (0/0) and hydrophobic + ionic interactions (15/15). (b) 10/10- and 20/20-hydrogels under compression (left) and elongation (right). (c) Compressive stress–strain curves of 15/15-hydrogels formed at various C18 contents.

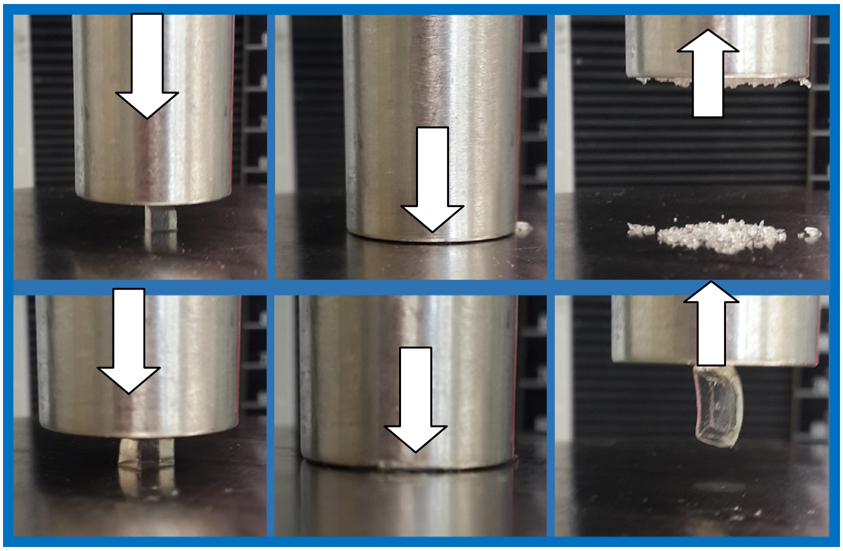

Fig. 5. Photographs of 15/15xl- (upper panel) and 15/15-hydrogel samples (bottom panel) before and after 99% compression, and after the release of the load.

ment. After waiting for 1 min at rest, the tests were repeated several times. Fig. 6a and b shows the results of successive compressive loading/unloading cycles conducted on 10/10-hydrogel specimens. The maximum compression ε_{max} was fixed at 80% in Fig. 6a while in Fig. 6b, it was stepwise increased from 20 to 80%. For clarity, the loading and unloading curves are shown by the solid and dotted lines, respectively. In both cases, the loading curve of the cycle differs from the unloading curve revealing the occurrence of a damage in the gels and energy dissipation during the cycle. Similar results were also obtained with the other hydrogels. The hysteresis energies U_{hys} of polyampholyte hydrogels calculated from the area between the compressive loading and unloading curves are shown in Fig. 6c and d as a function of the number of cycles and the maximum strain ε_{max}, respectively. For comparison, U_{hys} data of 0/0-hydrogel are also shown in Fig. 6c by the open symbols. Several interesting features can be seen from the figures:

(a) Increasing the ionic monomer content also increases the hysteresis energy U_{hys}. For instance, after the stepwise increase of ε_{max} from 20 to 80% compression, U_{hys} is 9, 19, and 24 kJ·m^{-3} for 10/10-, 15/15-, and 20/20-hydrogels. Because U_{hys} is related to the number of supramolecular bonds broken down during the mechanical cycle [35,36], the results reveal that increasing number of intermolecular non-covalent bonds are broken with increasing ionic monomer content.

(b) For a fixed maximum strain ε_{max} of 80%, U_{hys} of the 2nd cycle is 28 ± 12% smaller than the 1st cycle indicating that only a fraction of the bonds are irreversibly broken resulting in a permanent damage. However, the following cycles are nearly reversible with a constant hysteresis energy. For instance, U_{hys} of 10/10-hydrogel is 10.8 kJ·m^{-3} for the 1st cycle while in the following cycles it is constant at 7.8 ± 0.5 kJ·m^{-3}. The results thus indicate that around 30% of the physical bonds are irreversibly broken under strain while the remaining bonds reform by removing the strain.

(c) Because 0/0-hydrogel only contains hydrophobic associations, U_{hys} of this hydrogel is related to the energy due to the broken associations. Thus, it is possible to estimate the hysteresis energy contribution of the ionic interactions by subtracting U_{hys} of 0/0-hydrogel from U_{hys} of polyampholyte hydrogels. Calculations using the data in Fig. 6c reveal that the ionic bonds broken during the first compression cycle contributes to 31, 53, and 71% of the hysteresis energy for

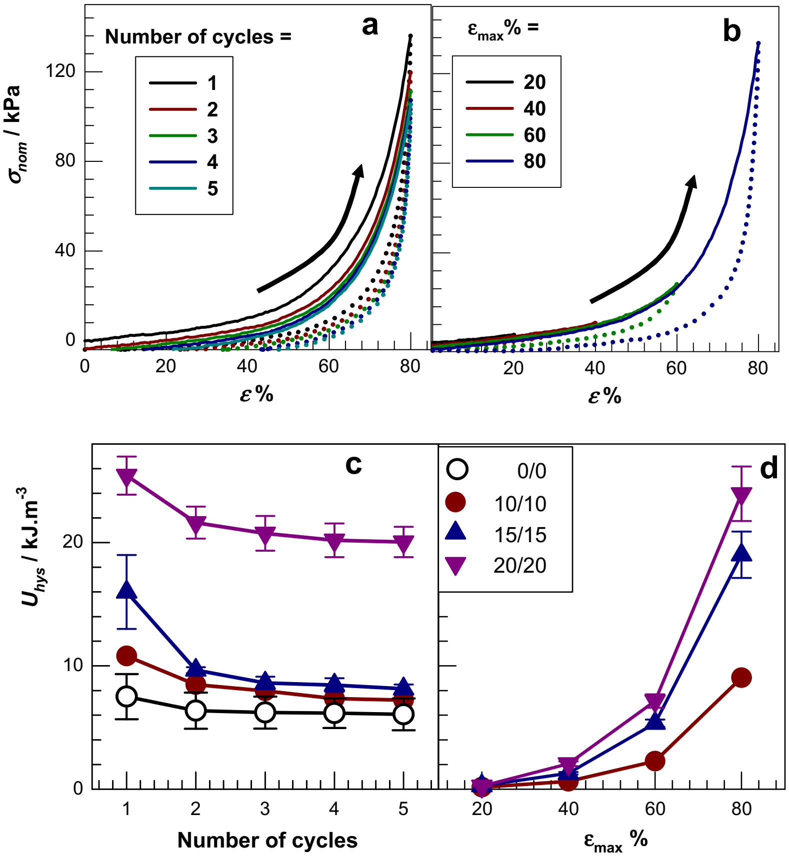

Fig. 6. Stress-strain curves from loading/unloading cyclic compression tests. (a and b) Successive compressive cycles up to ε_{max} = 80% (a), and with increasing ε_{max} from 20 to 80% conducted on 10/10-hydrogel samples. The loading and unloading curves are shown by the solid and dotted lines, respectively. (c and d): Hysteresis energies U_{hys} of polyampholyte hydrogels during successive compression cycles shown as a function of the number of cycles up ε_{max} = 80% (c), and the maximum strain ε_{max} (d). Open symbols in (c) represent the data of 0/0-hydrogels.

10/10-, 15/15-, and 20/20-hydrogels, respectively. Thus, both the hydrophobic associations and ionic bonds are broken under strain and increasing number of ionic segments in the network chains also increases the fraction of broken ionic bonds.

Similar results were also obtained by cyclic tensile tests conducted with increasing maximum tensile strain ε_{max} from 100 to 300% for 15/15- and 20/20-hydrogels (Fig. S3). As in the compression cycles, the first cycle was partially irreversible while the following cycles were nearly reversible with a constant hysteresis energy (Fig. S3).

Self-healing tests were conducted on hydrogel samples by cutting them into two pieces and then placing the cut surfaces together for various times up to 10 days at various temperatures between 23 and 50 °C. In contrast to the hydrogels formed via hydrophobic interactions in aqueous solutions [28,29], we could not observe any healing phenomena implying that the non-covalent interactions between the cut surfaces do not contribute to the self-healing. This finding is also in accord with the results of cyclic mechanical tests revealing the existence of irreversible broken bonds under large strain conditions.

3.3. Prediction of the pH inside the hydrogel by the theory of swelling equilibrium

The results presented so far show that the intermolecular electrostatic and hydrophobic interactions create hydrogels that are mechanically stronger than the chemically cross-linked ones. The supramolecular polyampholyte hydrogels exhibit up to 2-orders of magnitude change in the gel mass depending on the pH of the solution. Interestingly, they all assume a collapsed plateau over a wide range of pH and anti-polyelectrolyte behavior along the plateau pH (Fig. 2). The appearance of a plateau regime including the isoelectric point *pI* suggests that pH inside the hydrogel remains at the pH of *pI* although the external solution pH changes over a wide range [16,17]. To verify this presumption, in the following we use the classical Flory-Rehner swelling theory coupled to the Donnan equilibrium. According to the theory, the gel osmotic pressure π is the sum of three contributions [37]:

$$\pi = \pi_{mix} + \pi_{el} + \pi_{ion} \tag{1}$$

where π_{mix}, π_{el}, and π_{ion} are the mixing, elastic, and ionic contributions, respectively. Mixing contribution π_{mix} to the swelling pressure is obtained from the liquid-lattice theory of polymer solutions [37]:

$$\pi_{mix} = -\frac{RT}{\overline{V}_1}\left(\ln(1 - v_2) + v_2 + \chi v_2^2\right) \tag{2}$$

where R is the gas constant, T is the absolute temperature, $\overline{V}_1$ is the molar volume of solvent, v_2 is the volume fraction of cross-linked polymer in the equilibrium swollen gel, and χ is the polymer-solvent interaction parameter. Note that the polymer volume fraction v_2 is related to the experimentally determined swelling ratio q_w by

$$\upsilon_2 = \left[1 + (q_w - 1)\rho/d_1\right]^{-1} \tag{2a}$$

where ρ and d_1 are the densities of polymer and water, respectively. The elastic contribution π_{el} can be deduced from the statistical theory of rubber elasticity. Assuming phantom network behavior, it is given by [37,38]:

$$\pi_{el} = -0.5 v_e RT (v_2)^{1/3} (v_2^0)^{2/3} \tag{3}$$

where v_e is the cross-link density and v_2^0 is the volume fraction of cross-linked polymer at the state of gel preparation. In polyelectrolyte hydrogel systems, the ionic contribution π_{ion} to the gel swelling dominates over the mixing contribution π_{mix} due to the presence of mobile counterions, and is given by [37]:

$$\pi_{ion} = RT \sum_i (C_i^g - C_i^s) \tag{4}$$

where C_i is the molar concentration of the mobile ion *i* and the summation includes all mobile ions locating in the gel and in the surrounding solution, designated by superscripts *g* and *s*, respectively. The concentration difference $(C_i^g - C_i^s)$ of the mobile ion *i* between the gel and the solution is due to the fixed charges on the polyelectrolyte chains requiring an equivalent number of counterions to confine within the hydrogel to achieve electroneutrality. Polyampholyte hydrogel networks presented here are composed of non-ionic DMA and C18 segments together with weak electrolyte 4VP and AAc segments. The hydrogel is immersed in a reservoir of water containing H^+ (or OH^-), Na^+, and Cl^- ions. Defining the concentrations of the AAc and 4VP segments in the hydrogels by C_A and C_B, respectively, the conditions of the electroneutrality and Donnan equilibrium in and out of the gel are given by:

$$\alpha C_A + C_{Cl^-}^g = \beta C_B + C_{H^+}^g + C_{Na^+}^g \tag{5}$$

$$C_{H^+}^s + C_{Na^+}^s = C_{Cl^-}^s \tag{6}$$

$$C_{H^+}^g C_{Cl^-}^g = C_{H^+}^s C_{Cl^-}^s \tag{7}$$

$$C^g_{\mathrm{Na}^+}C^g_{\mathrm{Cl}^-} = C^s_{\mathrm{Na}^+}C^s_{\mathrm{Cl}^-} \tag{8}$$

Solution of the system of equations represented by Eqs. (5)–(8) gives the concentration difference of the mobile ions between the gel and the solution as:

$$\sum_i (C^g_i - C^s_i) = \sqrt{(\alpha C_A - \beta C_B)^2 + 4(C^s_{\mathrm{H}^+} + C^s_{\mathrm{Na}^+})^2} - 2(C^s_{\mathrm{H}^+} + C^s_{\mathrm{Na}^+}) \tag{9}$$

The dissociation degrees α and β of AAc and 4VP segments, respectively, relate to their dissociation constants K_a and K_b by:

$$\alpha = \frac{K_a}{K_a + C^g_{\mathrm{H}^+}} \tag{10a}$$

$$\beta = \frac{K_b}{K_b + K_w/C^g_{\mathrm{H}^+}} \tag{10b}$$

where K_w is the dissociation constant of water. Because the total osmotic pressure π is zero at the swelling equilibrium, using Eqs. (1)–(4) and (9), the equilibrium condition of a polyampholyte hydrogel immersed in an aqueous solution of NaCl and HCl is given by:

$$\ln(1 - v_2) + v_2 + \chi v_2^2 + 0.5 v_e \overline{V}_1 (v_2)^{1/3} (v_2^0)^{2/3} - \overline{V}_1\sqrt{(\alpha C_A - \beta C_B)^2 + (2C^s_{\mathrm{H}^+} + 2C^s_{\mathrm{Na}^+})^2} + 2\overline{V}_1(C^s_{\mathrm{H}^+} + C^s_{\mathrm{Na}^+}) = 0 \tag{11}$$

Solution of Eqs. (10) and (11) for the equilibrium swelling ratio of polyampholyte hydrogels requires hydrogen ion concentration inside the hydrogel $C^g_{\mathrm{H}^+}$, which may differ from that in the outer solution $C^s_{\mathrm{H}^+}$. By substituting Eqs. (10a–b) into (5), one may obtain a quartic equation for calculating $C^g_{\mathrm{H}^+}$:

$$C^{g\;4}_{\mathrm{H}^+} + (K_1 + C_B C_{rel})C^{g\;3}_{\mathrm{H}^+} + \left[K_2 + K_a(C_B - C_A)C_{rel} - C^{s\;2}_{\mathrm{H}^+}\right]C^{g\;2}_{\mathrm{H}^+} - (K_2 C_A C_{rel} + K_1 C^{s\;2}_{\mathrm{H}^+})C^g_{\mathrm{H}^+} - K_2 C^{s\;2}_{\mathrm{H}^+} = 0 \tag{12}$$

where $K_1 = K_a + K_w/K_b$, $K_2 = K_a K_w/K_b$, and $C_{rel} = C^s_{\mathrm{H}^+}/(C^s_{\mathrm{H}^+} + C^s_{\mathrm{Na}^+})$. The concentrations C_A and C_B of the AAc and 4VP segments, respectively, in the hydrogel are given by:

$$C_A = x_{AAc}\frac{v_2}{\overline{V}_r} \tag{13a}$$

$$C_B = x_{4VP}\frac{v_2}{\overline{V}_r} \tag{13b}$$

where $\overline{V}_r$ is the molar volume of polymer units. It should be mentioned that the presence of NaOH instead of HCl leads to the same equations except that the total concentration of HCl + NaCl in the external solution has to be redefined as that of NaOH + NaCl.

We solved Eqs. (10)–(13) numerically for both $\mathrm{pH_{in}}(= 10^{-C^g_{\mathrm{H}^+}})$ and q_w by taking pH and NaCl concentration of the solution as the independent parameters. The solution of the equations requires the values v_2^0, $\overline{V}_r$, v_e, and χ, describing the network characteristics and the extent of the polymer-water interactions. v_2^0 is equal to unity for the present hydrogels due to the bulk polymerization condition. Using the molecular weight of the monomers together with the polymer density (1.21 g/mL) [39], $\overline{V}_r$ was calculated as 82 mL·mol^{-1} for the polyampholyte hydrogels. The cross-link density v_e was estimated from the storage modulus G' of the hydrogels measured at ω = 140 rad·s^{-1} (Fig. 3). Assuming a homogeneous phantom network of Gaussian chains with tetrafunctional cross-links, v_e was estimated using the equation $G' = 0.5 v_e RT v_2^{1/3}$ as 21, 24, 36, and 74 mol.m^{-3} for 10/10-, 15/15-, 20/20-, and 15/15xl-hydrogels, respectively [38]. The χ parameter value for PDMA-water system was reported as $\chi = 0.47 + 0.36\ v_2$ [40].

Calculation results using Eqs. (10)–(13) are presented in Fig. 7a and b where the equilibrium swelling ratio q_w of the hydrogels in water and the pH inside the hydrogel ($\mathrm{pH_{in}}$) are shown as a function of pH of the solution. Fig. 7c and d shows q_w and pH_{in} for 15/15-hydrogel in equilibrium with aqueous solutions of NaCl at various concentrations between 0 and 1 M plotted against pH of the solution. Comparison of the theoretical curves with the experimental swelling data in Fig. 2 reveals that the theory qualitatively simulates the general trends observed by experiments. As compared to the chemically cross-linked 15/15xl hydrogel sample, supramolecular polyampholyte hydrogels exhibit a high degree of swelling at both low and high pH values. In accord with the experimental results, the hydrogels immersed in water are in a collapsed conformation over a range of pH including *pI*. The reason for the appearance of the plateau regime is seen in Fig. 7b: the $\mathrm{pH_{in}}$ remains constant at the *pI* values of the hydrogels although the solution pH changes between 4 and 8, thus covering 4-orders of magnitude change in H$^+$ concentration of the solution. Moreover, the addition of NaCl in the solution leads to deswelling of the hydrogels and the disappearance of the plateau regime. This is due to the screening of fixed charges and thus producing equimolar concentrations of H$^+$ ions both inside and outside the hydrogel.

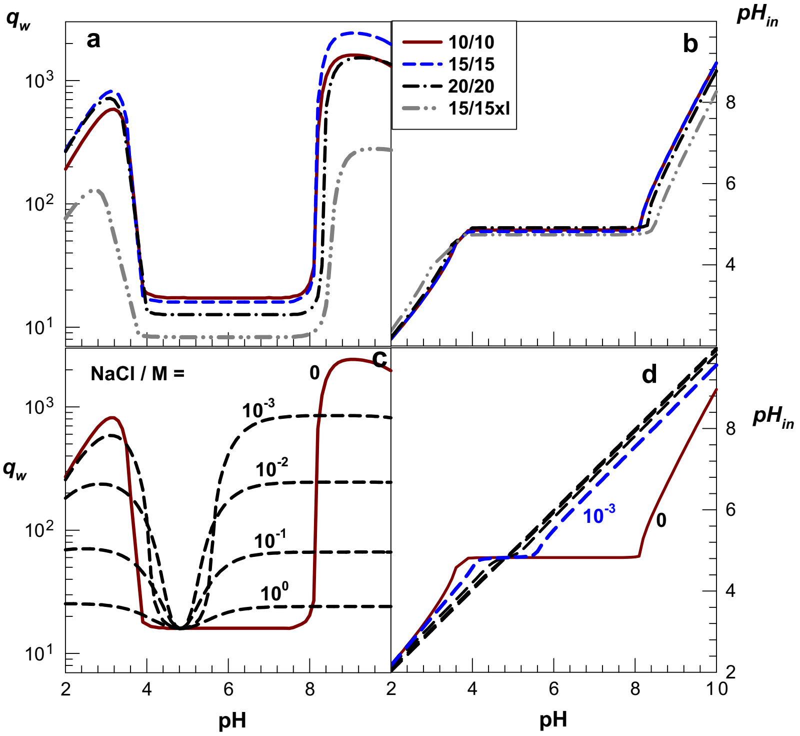

Fig. 7. (a, b) The equilibrium weight swelling ratio q_w of the hydrogels (a) and the pH in the gel (pH_{in}) (b) both plotted against the pH of the solution. The codes of the hydrogels are indicated. Calculations were using Eqs. (10)–(13). (c and d) q_w (c) and pH_{in} (d) of 15/15-hydrogel in equilibrium with water (solid curves) and in aqueous NaCl solutions (dashed curves) plotted against the pH of the solution.

The reason why pH within the hydrogel remains constant over a wide range of pH of the solution including *pI* can be explained using the concentrations of fixed and mobile ions in the hydrogels. Fig. 8 shows the concentrations of ionized AAc ($C_{\mathrm{AAc^-}}$) and 4VP segments ($C_{\mathrm{4VP^+}}$) together with H$^+$ concentration in the gel $C^g_{\mathrm{H^+}}$ at the *pI* of 15/15-hydrogel plotted against H$^+$ concentration of the solution$C^s_{\mathrm{H^+}}$.The concentrations of oppositely ionized AAc and 4VP segments are both 6.6×10^{-3} M along the plateau as compared to the H$^+$ concentration $C^g_{\mathrm{H^+}}$ of 1.4×10^{-5} M. Thus, the concentration of fixed charges is about 3-orders of magnitude larger than the H$^+$ concentration within the polyampholyte network. Because of

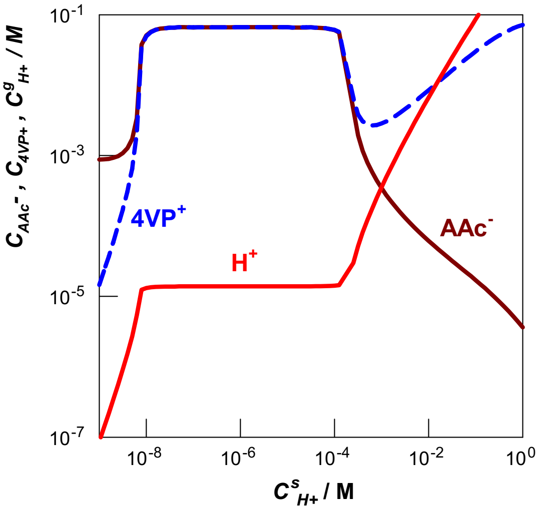

Fig. 8. Concentrations of ionized AAc ($C_{\mathrm{AAc^-}}$) and 4VP segments ($C_{\mathrm{4VP^+}}$), and H$^+$ concentration in the gel $C^g_{\mathrm{H^+}}$) at the *pI* of 15/15-hydrogel shown as a function of pH of the solution. Calculations were using Eqs. (10)–(13).

the deficiency of mobile ion concentration in the gel network, the condition of electroneutrality can only be provided by the electrostatic attractions between the fixed charges on AAc and 4VP segments. As seen in Fig. 7b, these attractions can be overcome by increasing external pH from 4 to 8, i.e., by creating 4-orders of magnitude H^+ concentration difference between the hydrogel and solution. We have to mention that the theory predicts much larger swelling ratios as compared to the experimental results due to the fact that the electrostatic interactions between ions and the effect of Mannich condensation are not accounted for in the theory.

4. Conclusions

Polyampholyte hydrogels were prepared by photopolymerization of the non-ionic monomer DMA, the hydrophobic monomer C18, and the ionic monomers AAc and 4VP under solvent-free condition. Equimolar amounts of AAc and 4VP between 10 and 20 mol% were used in the gel preparation together with the hydrophobic monomer C18 at a concentration of 2 mol% to create hydrophobic associations. The decrease of the swelling ratio and increase of the modulus of polyampholyte hydrogels with increasing content of ionic segments highlight the existence of electrostatic attractions between the copolymer chains acting as physical cross-link zones. The fact that polyampholyte hydrogels prepared in the absence of the hydrophobic comonomer C18 dissolve in water reveals the existence of hydrophobic associations between alkyl side chains of C18 segments contributing to the rubber elasticity of the hydrogels. In contrast to the chemically cross-linked polyampholyte hydrogel exhibiting frequency independent storage modulus, the supramolecular hydrogels exhibit frequency-dependent moduli and a loss factor above 0.1 demonstrating finite lifetimes of their physical cross-links. The results also show that intermolecular electrostatic and hydrophobic interactions create hydrogels that are mechanically stronger than the chemically cross-linked ones. From the cyclic mechanical tests, it is obvious that the hydrogels have both reversibly and irreversibly broken physical cross-links under large strain. The fraction of broken ionic bonds increases with increasing number of ionic segments in the hydrogels. The supramolecular polyampholyte hydrogels exhibit up to 2-orders of magnitude change in the gel mass depending on the pH of the solution. Moreover, they all assume a collapsed plateau over a wide range of pH including the isoelectric point and anti-polyelectrolyte behavior along the plateau regime. As demonstrated by the Flory-Rehner swelling theory coupled to the Donnan equilibrium, the appearance of a plateau regime is due to the fact that pH inside the hydrogel remains at the pH of the isoelectric point although the external solution pH changes over a wide range.

Acknowledgements

This work was supported by the Scientific and Technical Research Council of Turkey (TUBITAK), KBAG 114Z312. E.S. thanks TUBITAK-BIDEB for a PhD scholarship. O.O. thanks the Turkish Academy of Sciences (TUBA) for the partial support.

Appendix A. Supplementary material

Supplementary data associated with this article can be found, in the online version, at http://dx.doi.org/10.1016/j.eurpolymj.2017.01.029.

References

[1] J.T. Alfrey, H. Morawetz, E.B. Fitzgerald, R.M. Fuoss, Synthetic electrical analog of proteins, J. Am. Chem. Soc. 72 (1950). pp. 1864–1864.
[2] Katchalsky, I.R. Miller, Polyampholytes, J. Polym. Sci. 13 (1954) 57–68.
[3] C.S. Patrickios, W.R. Hertler, N.L. Abbott, T.A. Hatton, Diblock, ABC triblock, and random methacrylic polyampholytes: synthesis by group transfer polymerization and solution behavior, Macromolecules 27 (1994) 930–937.
[4] S.E. Kudaibergenov, Polyampholytes: Synthesis, Characterization and Application, Plenum, New York, 2002.
[5] A.B. Lowe, C.L. McCormick, Synthesis and solution properties of zwitterionic polymers, Chem. Rev. 102 (2002) 4177–4189.
[6] A.B. Lowe, C.L. McCormick (Eds.), Polyelectrolytes and Polyzwitterions: Synthesis, Properties and Applications, ACS Symposium Series, vol. 937, American Chemical Society, Washington, DC, 2006.
[7] S.E. Kudaibergenov, N. Nuraje, V.V. Khutoryanskiy, Amphoteric nano-, micro-, and macrogels, membranes and thin films, Soft Matter 8 (2012) 9302–9321.
[8] K.M. Zurick, M. Bernards, Recent biomedical advances with polyampholyte polymers, J. Appl. Polym. Sci. (2014), http://dx.doi.org/10.1002/app.40069.
[9] U.P. Strauss, Y.C. Chiao, Hydrophobic polyampholytes, Macromolecules 19 (1986) 355–358.
[10] N. Bonte, A. Laschewsky, Zwitterionic polymers with carbobetaine moieties, Polymer 37 (1996) 2011–2019.
[11] P. Kujawa, J.M. Rosiak, J. Selb, F. Candau, Synthesis and properties of hydrophobically modified polyampholytes, Mol. Cryst. Liq. Cryst. 354 (2000) 401–407.
[12] S.E. Kudaibergenov, A.G. Didukh, Z.E. Ibraeva, L.A. Bimendina, F. Rullens, M. Devillers, A. Laschewsky, A regular, hydrophobically modified polyampholyte as novel pour point depressant, J. Appl. Polym. Sci. 98 (2005) 2101–2118.
[13] J.P. Baker, D.R. Stephens, H.W. Blanch, J.M. Prausnitz, Swelling equilibria for acrylamide-based polyampholyte hydrogels, Macromolecules 25 (1992) 1955–1958.
[14] J.P. Baker, H.W. Blanch, J.M. Prausnitz, Swelling properties of acrylamide-based ampholytic hydrogels: comparison of experiment with theory, Polymer 36 (1995) 1061–1069.
[15] M. Annaka, T. Tanaka, Multiple phases of polymer gels, Nature 355 (1992) 430–432.
[16] S. Mafe, J.A. Manzanares, A.E. English, T. Tanaka, Multiple phases in ionic copolymer gels, Phys. Rev. Lett. 79 (1997) 3086–3089.
[17] S. Dogu, M. Kilic, O. Okay, Collapse of acrylamide-based polyampholyte hydrogels in water, J. Appl. Polym. Sci. 113 (2009) 1375–1382.

[18] M. Gao, K. Gawel, B.T. Stokke, Polyelectrolyte and antipolyelectrolyte effects in swelling of polyampholyte and polyzwitterionic charge balanced and charge offset hydrogels, Eur. Polym. J. 53 (2014) 65–74.

[19] L.R. Carr, H. Xue, S. Jiang, Functionalizable and nonfouling zwitterionic carboxybetaine hydrogels with a carboxybetaine dimethacrylate crosslinker, Biomaterials 32 (2011) 961–968.

[20] S.Q. Liu, C. Yang, Y. Huang, X. Ding, Y. Li, W.M. Fan, J.L. Hedrick, Y.-Y. Yang, Antimicrobial and antifouling hydrogels formed in situ from polycarbonate and poly(ethylene glycol) via Michael addition, Adv. Mater. 24 (2012) 6484–6489.

[21] L. Mi, S. Jiang, Synchronizing nonfouling and antimicrobial properties in a zwitterionic hydrogel, Biomaterials 33 (2012) 8928–8933.

[22] A.P. Constantinou, M. Elladiou, C.S. Patrickios, Regular and inverse polyampholyte hydrogels: a detailed comparison, Macromolecules 49 (2016) 3869–3880.

[23] Y. Fan, W. Zhou, A. Yasin, H. Li, H. Yang, Dual-responsive shape memory hydrogels with novel thermoplasticity based on a hydrophobically modified polyampholyte, Soft Matter 11 (2015) 4218–4225.

[24] T.L. Sun, T. Kurokawa, S. Kuroda, A.B. Ihsan, T. Akasaki, K. Sato, A. Haque, T. Nakajima, J.P. Gong, Physical hydrogels composed of polyampholytes demonstrate high toughness and viscoelasticity, Nat. Mater. 12 (2013) 932–937.

[25] A.B. Ihsan, T.L. Sun, T. Kurokawa, S.N. Karobi, T. Nakajima, T. Nonoyama, C.K. Roy, F. Luo, J.P. Gong, Self-healing behaviors of tough polyampholyte hydrogels, Macromolecules 49 (2016) 4245–4252.

[26] A. Lassoued, S. Djadoun, Elaboration and characterization of poly(4-vinylpyridine-co-N, N dimethylacrylamide)/poly(styrene-co-methacrylic acid) interpolymer complexes, Macromol. Symp. 336 (2014) 7–16.

[27] B. Li, X. Lu, Y. Ma, Z. Chen, Thermo- and pH-responsive behaviors of aqueous poly(acrylic acid)/poly(4-vinylpyridine) complex material characterized by ATR-FTIR and UV–Vis spectroscopy, Eur. Polym. J. 60 (2014) 255–261.

[28] D.C. Tuncaboylu, M. Sari, W. Oppermann, O. Okay, Tough and self-healing hydrogels formed via hydrophobic interactions, Macromolecules 44 (2011) 4997–5005.

[29] D.C. Tuncaboylu, M. Sahin, A. Argun, W. Oppermann, O. Okay, Dynamics and large strain behavior of self-healing hydrogels with and without surfactants, Macromolecules 45 (2012) 1991–2000.

[30] A. Argun, V. Can, U. Altun, O. Okay, Non-ionic double and triple network hydrogels of high mechanical strength, Macromolecules 47 (2014) 6430–6440.

[31] M.T.A. Ende, N.A. Peppas, Transport of ionizable drugs and proteins in crosslinked poly(acrylic acid) and poly(acrylic acid-co-2-hydroxyethyl methacrylate) hydrogels. I. Polymer characterization, J. Appl. Polym. Sci. 59 (1996) 673–685.

[32] A. Sugii, N. Ogawa, K. Harada, K. Nishimura, Metal sorption of macroreticular poly(4-vinylpyridine) resins cross-linked with oligo(ethylene glycol dimethacrylates), Anal. Sci. 4 (1988) 399–402.

[33] C.S. Patrickios, Polypeptide amino acid composition and isoelectric point: 1. A closed-form approximation, J. Colloid Interface Sci. 175 (1995) 256–260.

[34] U. Schroder, W. Oppermann, Properties of polyelectrolyte gels, in: J.P. Cohen Addad (Ed.), Physical Properties of Polymeric Gels, Wiley, NY, 1996, pp. 19–38.

[35] R.E. Webber, C. Creton, H.R. Brown, J.P. Gong, Large strain hysteresis and Mullins effect of tough double-network hydrogels, Macromolecules 40 (2007) 2919–2927.

[36] G.J. Lake, A.G. Thomas, The strength of highly elastic materials, Proc. R. Soc.: Lond. A 300 (1967) 108–119.

[37] P.J. Flory, Principles of Polymer Chemistry, Cornell University Press, Ithaca, NY, 1953 (Chapter 13).

[38] L.R.G. Treloar, The Physics of Rubber Elasticity, University Press, Oxford, 1975 (Chapter 7).

[39] N. Orakdogen, O. Okay, Effect of initial monomer concentration on the equilibrium swelling and elasticity of hydrogels, Eur. Polym. J. 42 (2006) 955–960.

[40] N. Gundogan, O. Okay, W. Oppermann, Swelling, elasticity and spatial inhomogeneity of poly(N,N-dimethylacrylamide) hydrogels formed at various polymer concentrations, Macromol. Chem. Phys. 205 (2004) 814–823.